AGU100 ADVANCING EARTH AND SPACE SCIENCE

Water Resources Research

RESEARCH ARTICLE
10.1029/2019WR025035

Key Points:
- We introduce the Climate State Intelligence framework to capture the state of multiple climate signals and improve seasonal forecast
- Strong influence of divergent SST patterns dependent on ENSO and NAO phases is detected over the Alpine region
- Preseason SST anomalies appear more valuable than hydrologic-based seasonal forecasts for informing reservoir operations

Supporting Information:
- Supporting Information S1

Correspondence to:
M. Giuliani,
matteo.giuliani@polimi.it

Citation:
Giuliani, M., Zaniolo, M., Castelletti, A., Davoli, G., & Block, P. (2019). Detecting the state of the climate system via artificial intelligence to improve seasonal forecasts and inform reservoir operations. *Water Resources Research*, *55*, 9133–9147. https://doi.org/10.1029/2019WR025035

Received 21 FEB 2019
Accepted 9 OCT 2019
Accepted article online 20 OCT 2019
Published online 16 NOV 2019

Detecting the State of the Climate System via Artificial Intelligence to Improve Seasonal Forecasts and Inform Reservoir Operations

Matteo Giuliani[1], Marta Zaniolo[1], Andrea Castelletti[1], Guido Davoli[2,3], and Paul Block[4]

[1]Department of Electronics, Information, and Bioengineering, Politecnico di Milano, Milan, Italy, [2]Department of Economics, Cà Foscari University, Venice, Italy, [3]Centro Euro-Mediterraneo sui Cambiamenti Climatici (CMCC), Bologna, Italy, [4]Department of Civil and Environmental Engineering, University of Wisconsin-Madison, Madison, WI, USA

Abstract Increasingly variable hydrologic regimes combined with more frequent and intense extreme events are challenging water systems management worldwide. These trends emphasize the need of accurate medium- to long-term predictions to timely prompt anticipatory operations. Despite in some locations global climate oscillations and particularly the El Niño Southern Oscillation (ENSO) may contribute to extending forecast lead times, in other regions there is no consensus on how ENSO can be detected, and used as local conditions are also influenced by other concurrent climate signals. In this work, we introduce the Climate State Intelligence framework to capture the state of multiple global climate signals via artificial intelligence and improve seasonal forecasts. These forecasts are used as additional inputs for informing water system operations and their value is quantified as the corresponding gain in system performance. We apply the framework to the Lake Como basin, a regulated lake in northern Italy mainly operated for flood control and irrigation supply. Numerical results show the existence of notable teleconnection patterns dependent on both ENSO and the North Atlantic Oscillation over the Alpine region, which contribute in generating skilful seasonal precipitation and hydrologic forecasts. The use of this information for conditioning the lake operations produces an average 44% improvement in system performance with respect to a baseline solution not informed by any forecast, with this gain that further increases during extreme drought episodes. Our results also suggest that observed preseason sea surface temperature anomalies appear more valuable than hydrologic-based seasonal forecasts, producing an average 59% improvement in system performance.

1. Introduction

Increasingly variable hydrologic regimes combined with more and more frequent and intense extreme events are challenging water systems management worldwide (Dai, 2011; Trenberth, 2011). Additional pressures generated by global trends in population growth and rising economic prosperity are expected to increase the demand for energy, food, and water (Padowski et al., 2015; Rodell et al., 2018). These variable and evolving conditions require further flexibility of water systems operations to activate early actions and decisions, possibly informed by accurate medium- to long-term predictions (Benson, 2016; Ziervogel et al., 2010).

Most existing water systems are currently operated with static rules conditioned on basic information systems including the day of the year and the storage, and, in few cases, also the previous day inflow (Hejazi et al., 2008). Yet the utility of forecasts in reservoir operations has long been recognized (e.g., Faber & Stedinger, 2001; Kelman et al., 1990; Kim & Palmer, 1997), and recent studies illustrate promising applications using hydrologic forecasts spanning variable time scales (e.g., Anghileri et al., 2016; Lu et al., 2017; Nayak et al., 2018; Turner et al., 2017), possibly conditioned on global climate oscillations (e.g., Gelati et al., 2011; Giuliani & Castelletti, 2019; Libisch-Lehner et al., 2019). Hydrologic forecasts are typically generated via either dynamic, process-based climate models (see Yuan et al., 2015, and references therein) with outputs (e.g., precipitation and temperature) fed into hydrologic models (Cloke & Pappenberger, 2009), or via empirical, data-driven models (Block & Rajagopalan, 2007; Sharma, 2000), which produce either meteorological

forecasts to feed hydrologic models or directly predict future streamflows. However, neither approach has been shown to consistently outperform the other, with dynamic models often limited by resolutions and initialization procedures (Georgakakos et al., 2004) and empirical models constrained by short observational records and stationarity assumptions (Block & Goddard, 2012).

Both dynamic and empirical forecast models generally rely on variability in sea surface temperature (SST) as the main source of predictability at seasonal or longer lead times (Palmer & Hagedorn, 2006). However, the contribution of global climate oscillations to local predictability depends on the degree to which local conditions are affected by these global climatic anomalies. The El Niño Southern Oscillation (ENSO) is generally considered the dominant interannual signal of global climate variability (McPhaden et al., 2006; Ward et al., 2010, 2014). ENSO is a coupled ocean-atmosphere phenomenon observed over the tropical Pacific Ocean with a 2- to 7-year period, with El Niño representing the oceanic component and Southern Oscillation the atmospheric one (Sarachik & Cane, 2010). In normal conditions the Walker circulation determines the atmospheric circulation over the tropical Pacific with trade winds blowing westward and moving warm moist air and warm surface water toward the western Pacific while keeping the central and eastern Pacific relatively cool. During an El Niño event, trade winds weaken or may even reverse, allowing the warm water from the western Pacific to move into the central and eastern tropical Pacific. Droughts in Indonesia and eastern Australia become far more common during El Niño events, while rainfall falls on the normally arid coasts of Perù and Equador. La Niña events are characterized by an intensification of the Walker circulation, with greater convection over the western Pacific and stronger trade winds, usually associated with exceptionally warm and wet conditions in the the western part of the tropical Pacific Ocean while the eastern part turns cool and dry. The ENSO teleconnection is therefore well defined in some locations, such as the United States (e.g., Grantz et al., 2007; Hamlet & Lettenmaier, 1999; Kahya & Dracup, 1993), western South America (e.g., Grimm & Tedeschi, 2009; Poveda et al., 2011), or Australia (e.g., Chiew et al., 2003; Sharma et al., 2000). Yet little to no consensus exists on how ENSO influences other regions, including Europe, where local conditions depend on the concurrent state of other climate signals (Steirou et al., 2017; Zanchettin et al., 2008), particularly the North Atlantic Oscillation (NAO; e.g., Kingston, Lawler, et al., 2006; Kingston, McGregor, et al., 2006).

In this paper, we propose a novel framework called Climate State Intelligence (CSI), which aims to use artificial intelligence for producing seasonal hydrologic forecasts based on multiple global climate signals and assessing their value on operational decisions (Figure 1). The use of multiple climate signals ensures the portability of this framework to different geographic locations, including regions where traditional teleconnections are weak. The framework extends the Nino Index Phase Analysis (NIPA) originally proposed by Zimmerman et al. (2016) to enable capturing the concurrent state of multiple climate signals, such as ENSO and NAO. Adopting an empirical, data-driven approach based on multivariate Extreme Learning Machine (ELM) models (Huang et al., 2006), we use the detected teleconnections and other observed preseason SST anomalies to forecast local meteorological variables on a seasonal time scale. The resulting forecasts are subsequently transformed using a dynamic hydrologic model into streamflow predictions, which are used as additional inputs for informing water systems operations. Finally, we apply the Information Selection and Assessment (ISA) framework proposed by Giuliani et al. (2015) to compute the value of the generated hydrologic forecasts with respect to a baseline solution that does not use any forecast information.

However, while hydrologic (i.e., streamflow) forecasts might be an intuitive approach to improving water reservoir operations (e.g., Block, 2011; Georgakakos & Graham, 2008), they require a chain of models that also introduces modeling errors and forecast biases, which may diminish the estimated operational value. This prompts the following key questions: Do we really need forecast models to make better decisions? Do hydrologic forecasts necessarily lead to superior reservoir operations? Can the original (observed) sources of predictability (e.g., preseason SST) be as valuable as the hydrologic forecast model outputs? To address these questions, we compare the operational value of the hydrologic forecast with two alternative pieces of information produced in the first two steps of our framework: (i) the seasonal meteorological forecasts, which only require the precipitation forecast model and eliminate the hydrologic model biases, and (ii) the observed preseason SSTs, which remove the entire forecast model chain.

We apply the CSI framework to the Lake Como basin, a regulated lake in northern Italy, which is mainly operated for flood control and irrigation supply. The lake catchment, located in the Italian lake district, is characterized by a mixed snow- and rain-dominated hydrology (Giuliani, Castelletti, et al., 2016). Despite

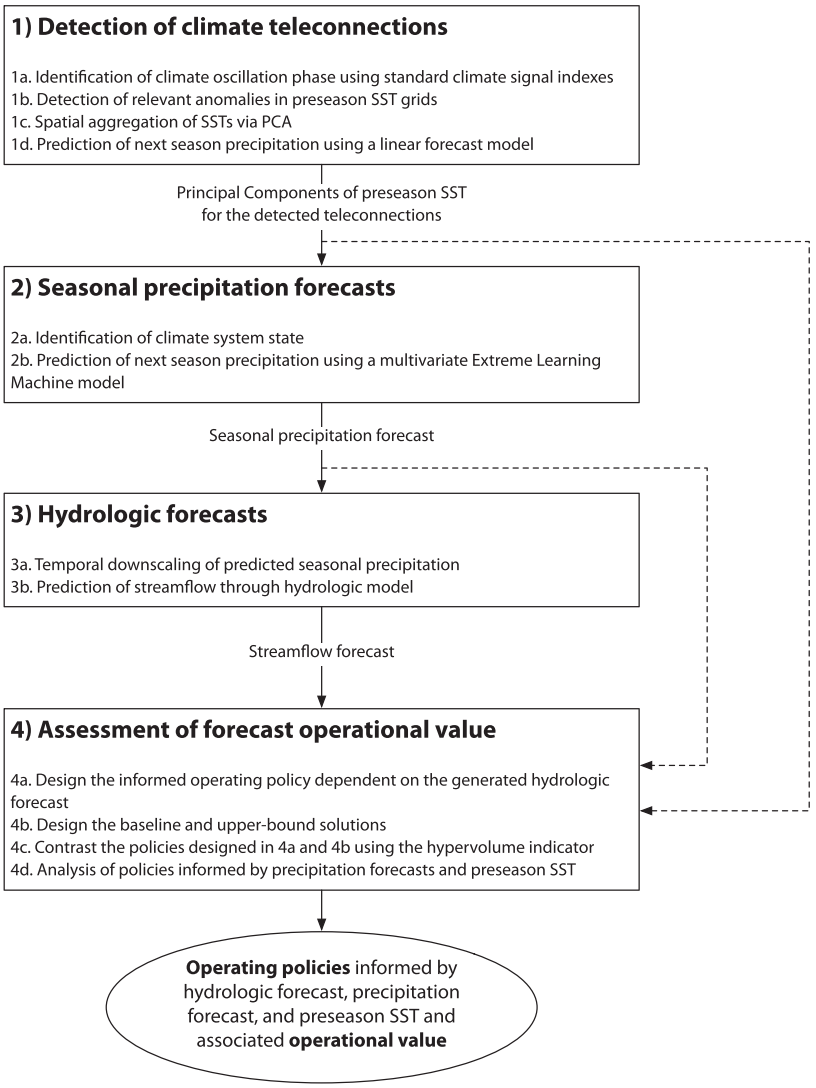

Figure 1. Overview of the Climate State Intelligence framework for the generation of seasonal hydrologic forecasts based on global climate oscillations and the assessment of their operational value. The dashed lines represent the operational value assessment of the outputs produced in the first two steps of the framework.

expected benefits to seasonal irrigated agriculture (Denaro et al., 2017), the lack of recognized teleconnections in this region has historically limited the skill of seasonal forecasts (Li et al., 2017), precluding their integration into the lake regulation, which, today, is simply informed by the day of the year and the lake level (Denaro et al., 2017; Todini, 2014). A number of studies investigate the correlation between NAO phases and snow dynamics in the Alpine region (e.g., Beniston, 1997; Scherrer et al., 2004) and suggest that the negative phase of NAO is typically associated with above average temperature and precipitation in Southern Europe, leading to more liquid than solid winter precipitation and accelerated melting processes. Other studies, however, conclude that the role of NAO in the Alpine region is marginal (e.g., Durand et al., 2009; López-Moreno et al., 2011). A lack of consensus also exists regarding ENSO teleconnections; some studies suggest significant correlations in the region (e.g., Brandimarte et al., 2011; Folland et al., 2009), while others find marginal ENSO influence (e.g., Bartolini et al., 2009; Efthymiadis et al., 2007; Shaman, 2014).

In summary, this paper provides a threefold contribution: (i) The application to the Lake Como system advances the understanding of hydroclimatic variability in the Alpine region and its dependency on global climate oscillations; (ii) the CSI framework introduces a formalized procedure to quantify the role of the propagation of error introduced by forecast models with respect to the forecast operational value; and

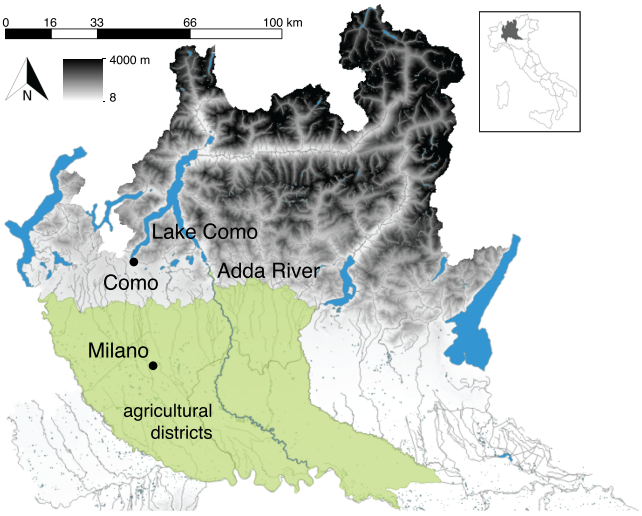

Figure 2. Map of the Lake Como basin.

(iii) our framework provides an emblematic demonstration for the potential of Artificial Intelligence tools in supporting water management during extreme events (Rolnick et al., 2019).

2. Study Site

Lake Como is a subalpine lake in the Italian lake district, northern Italy (Figure 2). It is the third-largest lake in Italy and reaches a maximum depth of 410 m, which makes it the fifth-deepest lake in Europe. The lake is shaped like an inverted "Y" surrounded by mountains and primarily fed by the Adda River, which also serves as the only exit point of the lake. The lake catchment has an area of 4,733 km^2, with approximately 90% in Italy and 10% in Switzerland. The hydrologic regime is snow-rainfall dominated, characterized by relatively dry winters and summers and high peaks of flow in spring and autumn, due to snowmelt and rainfall, respectively.

The Lake Como system involves numerous economic activities and has been actively studied since the 1980s (e.g., Guariso et al., 1984, 1986). The existing regulation of the lake is driven by two primary, competing objectives: water supply, mainly for irrigation, and flood control in the city of Como, which sits at the lowest point on the lake shoreline. The agricultural districts downstream prefer to store snowmelt in the lake to satisfy the peak summer water demands, when the natural inflow is insufficient to meet irrigation requirements. Yet storing such water increases the lake level and, consequently, the flood risk, which could instead be minimized by keeping the lake level as low as possible. On the basis of previous works (e.g., Castelletti et al., 2010; Denaro et al., 2017; Giuliani & Castelletti, 2016; Giuliani, Castelletti, et al., 2016), these two objectives (both to be minimized) are formulated as follows:

- *Flood control* (J^F): the average annual number of flooding days in the simulation horizon.
- *Water supply deficit* (J^D): the daily average quadratic water deficit between lake releases and downstream water demands, subject to a minimum environmental flow constraint to ensure adequate environmental conditions in the Adda River. This quadratic formulation aims to penalize severe deficits in a single time step, while allowing for more frequent, small shortages (Hashimoto et al., 1982).

Further details about the Lake Como integrated model and policy design problem formulation are provided in section S1 of the supporting information.

3. Methodology

Our CSI framework is composed of four steps as illustrated in Figure 1:

1. The detection of relevant climate teleconnections is performed by means of NIPA (Zimmerman et al., 2016), which analyzes independently multiple climate signals; categorizes the available years looking at the climate oscillation phase; and, for each phase, identifies preseason SST anomalies statistically significantly correlated with local conditions.
2. The seasonal precipitation forecasts are generated by capturing multiple climate signals using a nonlinear, multivariate ELM model (Huang et al., 2006), which is conditioned on the preseason SST for the relevant teleconnections detected in the previous step.
3. The hydrologic forecasts are produced through a temporal downscaling procedure of the seasonal precipitation forecast to feed a hydrologic model.
4. The forecast operational value is assessed by using the ISA framework proposed by Giuliani et al. (2015).

Details about each step of the framework are reported in the next subsections.

3.1. Detection of Climate Teleconnections

The first step of our framework relies on NIPA, a statistical framework originally developed by Zimmerman et al. (2016) for predicting seasonal precipitation conditioned on prior season atmospheric-oceanic variables. In contrast to other studies that use the state of ENSO as a predictor in their models, this technique expresses ENSO as a physical influence on the "mean state" of the ocean-atmosphere

system, in order to uncover possible asymmetric relationships (e.g., if in a given river basin El Niño is associated with dry conditions, La Niña not necessarily associates with wet conditions) that may be informative in a statistical prediction framework but are often overlooked. The NIPA methodology groups the available years into different phases (e.g., positive and negative if two phases are selected) according to the state of a climate signal (e.g., ENSO or NAO) as measured by its corresponding index. Subsequently, phase-specific SST fields are identified and used as predictors in a seasonal forecast model. Each phase is then evaluated individually, thus constructing as many predictive models as the number of phases.

The first step of the modeling procedure consists of identifying the most significant SST predictor regions for each phase of the climate signal. For this purpose, correlation maps between the seasonal mean of local precipitation and preseason SST anomaly patterns are used, and correlated regions at the 95% significance level are identified for each phase. A Monte Carlo test is performed to ensure that SST grids are not randomly selected (i.e., SST grids must be present at the 95% significance level 90% of the time to be included). After identifying the SST predictor regions, a Principal Component Analysis (PCA; see Joliffe, 2002) is conducted on the entire predictor field, and the first m resulting Principal Components (PCs) are retained as predictors in the forecast model. As in Zimmerman et al. (2016), we considered only the first PC of preseason SST for each phase ($PC^1_{\tau-1}$), as it generally explains most of the variance in the selected SST predictor regions. The linear forecast model is defined as follows:

$$\hat{y}_\tau = \beta * PC^1_{\tau-1} + \alpha, \tag{1}$$

where $\hat{y}_\tau$ is the predicted seasonal local precipitation, β the regression coefficient, and α the intercept. Given the low year-to-year persistence in precipitation data, a leave-one-out cross-validation procedure is then applied to the linear model to avoid model overfitting, and predictive skill is measured with the Pearson correlation coefficient. Additional details on the NIPA framework are provided in section S2.

3.2. Seasonal Precipitation Forecasts

The second step of our framework constructs an empirical multivariate forecast model from the NIPA results. The teleconnections detected in the previous step are used for grouping the years into distinct climate states defined as combinations of the original phases of each climate signal. For example, the positive and negative phases of ENSO and NAO would combine to four climate states (i.e., positive-positive, positive-negative, negative-positive, and negative-negative). Including a neutral phase is also possible, although this results in nine climate states and may create challenges due to the limited length of available data.

The multivariate forecast model is defined as a function of the first PC extracted from the preseason SST of each climate signal, along with a categorical flag indicating the climate state. We tested different data-driven model classes, including linear models, Artificial Neural Networks (ANNs), and ELMs. The latter is a model belonging to the family of ANNs that bypass the time-consuming gradient-based search of optimal ANN parameters by defining randomly parameterized hidden nodes and subsequently optimizing only their output weights through a one-step matrix product (Huang et al., 2006). Numerical results suggest that ELMs outperform the other models (for details, see Table S1). The multivariate ELM forecast model is hence formulated as

$$\hat{y}_\tau = ELM(PC^{1,S1}_{\tau-1}, PC^{1,S2}_{\tau-1}, \gamma) = \sum_{i=1}^{N} w_i \psi_i(PC^{1,S1}_{\tau-1}, PC^{1,S2}_{\tau-1}, \gamma, \xi_i), \tag{2}$$

where $\hat{y}_\tau$ is the predicted seasonal local precipitation, $PC^{1,S1}_{\tau-1}$ and $PC^{1,S2}_{\tau-1}$ are the first PCs of preseason SST for two climate signals (e.g., ENSO and NAO); γ is a categorical climate-state flag; N is the number of nonlinear nodes in the hidden nodes ψ_i, each using a sigmoidal activation function characterized by randomly generated (and thus not calibrated) parameters ξ_i; and w_i are the outputs weights to be calibrated.

3.3. Hydrologic Forecasts

The third step of our framework generates hybrid hydrologic forecasts by transforming the seasonal precipitation forecasts produced by the ELM model into streamflow forecasts using a hydrologic model. This step requires temporal disaggregation of the predicted seasonal precipitation to an appropriate resolution for running the hydrologic model. Similarly to Souza Filho and Lall (2003), temporal disaggregation is performed by means of the k-Nearest Neighbor (kNN) resampling method (Nowak et al., 2010). This data-driven method

captures the observed variability, is consistent with the lag correlation structures in the observed data, and ensures mass conservation and continuity at the daily time scale (Rajagopalan et al., 1997). The temporal disaggregation relies on the computation of a seasonal proportion matrix P_t^τ, which distributes the seasonal precipitation volume over all days t within season τ. Then, kNNs of the seasonal precipitation are identified from the historical record. Finally, one of the neighbors is randomly selected according to a probability distribution that is proportional to the similarity of the historical season with the predicted one.

The disaggregated precipitation forecasts are used as inputs to a hydrologic model. Specifically, we use the well-known conceptual hydrologic model Hydrologiska Byrans Vattenbalansavdelning (HBV; see Lindström et al., 1997), originally developed for operational flood forecasting in Sweden, which relies on four storage units, one for snow, and the other three for different soil layers.

3.4. Assessment of Forecast Operational Value

The last step of our framework assesses the operational value of the hydrologic forecasts, defined as the difference in system performance between an operating policy that uses the forecast information I_t (e.g., the hydrologic forecasts), and a baseline operating policy relying on more traditional information, such as the day of the year d_t and the lake level h_t, which in the case of Lake Como is sufficient to reproduce 85% of the variance of the observed release time series (Denaro et al., 2017). According to the ISA framework (Giuliani et al., 2015), this analysis also includes an upper-bound solution, designed assuming perfect foresight of future inflows, which allows estimating the potential maximum improvement of baseline operations. Additional details on the ISA framework are provided in section S4.

The optimal operating policies are computed by solving a multiobjective optimal control problem (Castelletti et al., 2008) formulated as follows:

$$p^* = \arg\min_p \mathbf{J} = |J^F, J^D|, \tag{3}$$

where the closed loop control policy p determines the release decision $u_t = p(d_t, h_t, I_t)$ at each time step t over the simulation horizon and the operating objectives are described in section 2. Note that the problem in equation (3) does not yield a unique optimal solution but a set of Pareto optimal solutions $\mathcal{P}^*$. The image in the objective space of the Pareto-optimal solutions is the Pareto front $\mathcal{F}$. To allow the direct use of hydrological forecasts as policy input, the problem in equation (3) is solved by using the Evolutionary Multi-Objective Direct Policy Search method (Giuliani, Castelletti, et al., 2016), which implements a data-driven control strategy by integrating direct policy search, nonlinear approximating networks, and multiobjective evolutionary algorithms.

Given the Pareto optimal solutions of the problem in equation (3), the operational value of the hydrologic forecast is quantified by the hypervolume indicator (HV), which captures both the convergence of the Pareto front conditioned on forecast information $\mathcal{F}$ to the ideal one assuming perfect foresight of future inflows $\mathcal{F}'$ as well as the representation of the full extent of trade-offs in the objective space (Zitzler et al., 2003). The hypervolume measures the objective space volume dominated ($\preccurlyeq$) by the considered set of solutions and HV is calculated as the hypervolume ratio between $\mathcal{F}$ and $\mathcal{F}'$, formally defined as follows (for a visual representation, see Figure S4a):

$$HV(\mathcal{F}, \mathcal{F}') = \frac{\int \alpha_{\mathcal{F}}(\mathbf{x})dx}{\int \alpha_{\mathcal{F}'}(\mathbf{x})dx} \quad \text{where}$$
$$\alpha_{\mathcal{F}}(\mathbf{x}) = \begin{cases} 1 \text{ if } \exists \mathbf{x}' \in \mathcal{F} \text{ such that } \mathbf{x}' \preccurlyeq \mathbf{x} \\ 0 \text{ otherwise.} \end{cases} \tag{4}$$

This metric allows set-to-set evaluations, with HV assuming values between 0 to 1. Larger HV values imply superior Pareto optimal sets, with $HV = 1$ assigned to the set of upper-bound solutions relying on perfect forecast information.

3.5. Data and Experimental Settings

The historical precipitation data used in this study are taken from Euro4M-APGD (i.e., Alpine Precipitation Gridded Dataset) developed by MeteoSwiss in the framework of the EURO4M (European Reanalysis and Observations for Monitoring deliverables) project. The data consist of a quality controlled, gridded data set of daily precipitation from 1971 to 2008, which extends over the entire Alpine region and is based on measurements from high-resolution rain-gauge networks, encompassing more than 8,500 stations from Austria,

Croatia, France, Germany, Italy, Slovenia, and Switzerland. For more information, see Isotta et al. (2014). Global Sea Surface Temperature anomalies were obtained from the NOAA's Extended Reconstructed SST (ERSST) Version 3b, a global monthly gridded data set with a spatial resolution of 2.5°.

We consider five candidate climate signals for improving the seasonal prediction of the precipitation in the Lake Como basin, including ENSO, NAO, Pacific Decadal Oscillation, Atlantic Multidecadal Oscillation, and Indian Ocean Dipole. To distinguish the phases of different signals, we use the Multivariate ENSO Index (MEI) from NOAA, the Station-based Hurrell NAO Index from the National Center for Atmospheric Resource, along with the PDO Index, the AMO Index, and the Dipole Mode Index all from KNMI. The MEI is an index calculated based on the six main observed variables over the tropical Pacific: sea level pressure, zonal and meridional components of the surface wind, SST, surface air temperature, and total cloudiness fraction of the sky (for details, see Wolter & Timlin, 1998). The NAO index is instead defined as the difference between the normalized mean winter (December–March) sea level pressure anomalies at Lisbon (Portugal) and Stykkisholmur (Iceland; Hurrell & Van Loon, 1997). The PDO Index is defined as the leading PC of North Pacific monthly SST variability (poleward of 20° N for the 1900–1993 period). The AMO Index is defined as the SST average over 0°–60°N, 0°–80°W minus the SST average over 60°S to 60°N. The DMI Index is an indicator of the east-west temperature gradient across the tropical Indian Ocean, which is calculated as the difference of the Western Tropical Indian Ocean SST index and the South Eastern Tropical Indian Ocean SST index.

To solve the policy design problem via Evolutionary Multi-Objective Direct Policy Search, the policies are defined as Gaussian radial basis functions, which have been demonstrated to be effective in solving these types of multiobjective policy design problems (Giuliani, Castelletti, et al., 2016). The policy parameters are optimized using the self-adaptive Borg MOEA (Hadka & Reed, 2013), which has been shown to be highly robust in solving multiobjective optimal control problems (Zatarain-Salazar et al., 2016). Each optimization was run for 2 million function evaluations over the simulation horizon 1996–2008, which was selected because it shows good variability in the local hydrological conditions including some intense droughts events. This time horizon is used for both the optimization and evaluation of the policy performance, which is hence likely overestimated as not tested on out-of-sample observations. However, the Lake Como inflows have already manifested a nonstationary trend over the last decades (see Giuliani, Li, et al., 2016). The droughts of 2003-2005-2006, all used for the optimization of the policies as representative of extreme drought events, are therefore unprecedented and prevent using the 1971–1995 horizon for validating the policy performance as this latter is much wetter than the most recent years. To improve solution diversity and avoid dependence on randomness, the solution set from each formulation is the result of 20 random optimization trials. The final set of Pareto optimal policies for each experiment is defined as the set of nondominated solutions from the results of all the optimization trials.

Finally, we provide a more tangible measure of the forecast operational value by converting the water supply deficit J^D into monetary values by using a spatially distributed agricultural model of the Muzza irrigation district, the largest district served solely by Lake Como releases. This model simulates soil-crop water balance (Facchi et al., 2004), crop growth stages as a function of the heat units accumulated (Neitsch et al., 2011), and final crop yield accounting for the effects of stresses due to insufficient water supply that may have occurred during the agricultural season (Steduto et al., 2009). Further details about the different model components are provided in section S1.

Source code is available on Github: NIPA and ELM (https://github.com/mxgiuliani00/CSI), HBV model (https://github.com/mxgiuliani00/hbv), and Lake Como simulation and EMODPS implementation (https://github.com/mxgiuliani00/LakeComo).

4. Results

4.1. Detection of Climate Teleconnections

In the first step of the CSI framework (Figure 1), we run NIPA to detect the presence of potential teleconnections between multiple climate signals with the local precipitation in the Lake Como basin. We report here only results for ENSO and NAO related to wintertime precipitation (seasonal average precipitation in January, February, and March, mainly as snow, which is highly correlated with spring inflows to the lake generated by the melting of the snow stored during the winter months on the mountains), which provide the

Table 1
Pearson Correlation Coefficients Between Predicted and Observed Winter Precipitation P_{JFM} with Associated Level of Confidence for Each Phase of NAO and ENSO (Predictions Depend on Preseason SST Anomalies)

Climate signal	Phase	Pearson correlation	Level of confidence
NAO	Negative	0.50	89.00%
	Positive	0.52	69.70%
ENSO	Negative	0.41	32.00%
	Positive	0.51	96.20%

best predictions of seasonal precipitation using the linear model in equation (1). Results for other climate signals and other seasons are reported in the supporting information (see Tables S2 and S3).

Wintertime predictions from preseason SST anomalies conditioned on the NAO negative phase and the ENSO positive phase independently result in high Pearson correlation values and high levels of confidence (Table 1). In particular, the prediction of winter precipitation obtained with the NAO negative phase has a correlation value of 0.50 with a level of confidence equal to 0.89; the positive phase of ENSO has a correlation value of 0.51 with a level of confidence equal to 0.96. These values of correlation are significantly higher than a standard regression model that is constructed without separating NAO and ENSO phases (Pearson correlation equal to 0.34), warranting the adoption of NIPA for the detection of climate teleconnections with asymmetric relationships with the local hydroclimatic processes.

Figure 3 illustrates the preseason SST grids selected by NIPA when exploring ENSO and NAO teleconnections (i.e., running a global search for preseason SST anomalies correlated with the seasonal precipitation in the Lake Como basin splitting the data according to the positive and negative phase of each climate signal). The selected spatial extent of SST patterns is larger for the negative phase of NAO and the positive phase of ENSO than for the opposite phases, further indicating an asymmetric influence of the two climate signals during these phases. In particular, SST anomalies negatively correlated with winter precipitation during the negative phase of NAO are located in the western equatorial and North Pacific Ocean, in the eastern equatorial Atlantic Ocean, and in a small area in the central Indian Ocean. Positive correlations are evident in

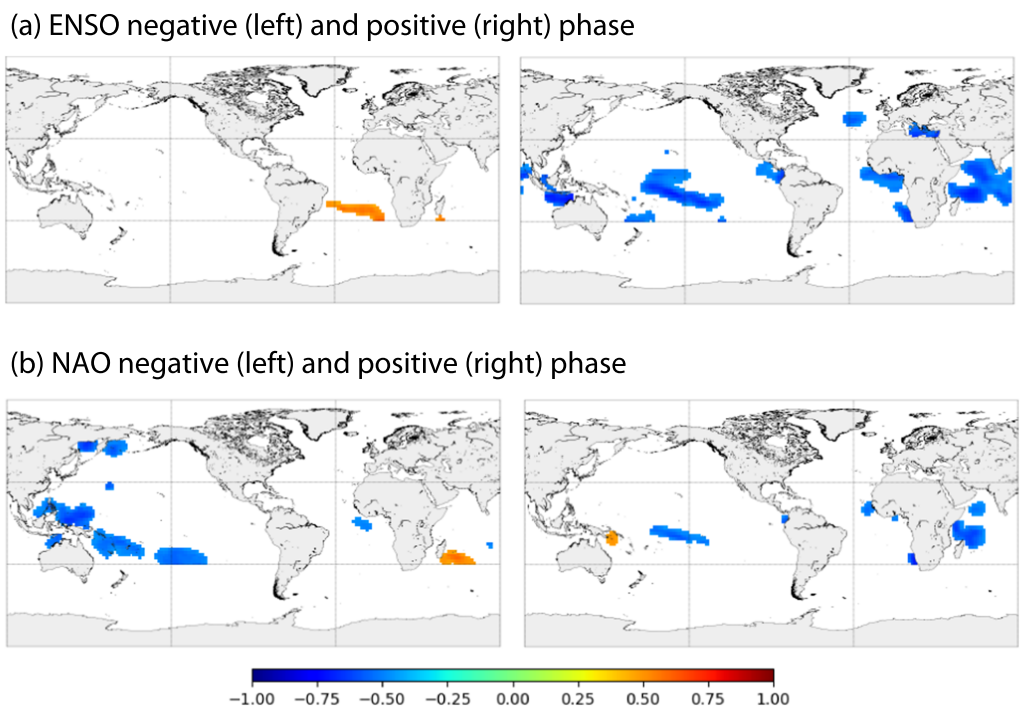

Figure 3. Correlation maps between October, November, and December SST anomalies and January, February, and March precipitation in the Lake Como catchment for the two phases of ENSO (panel a) and NAO (panel b).

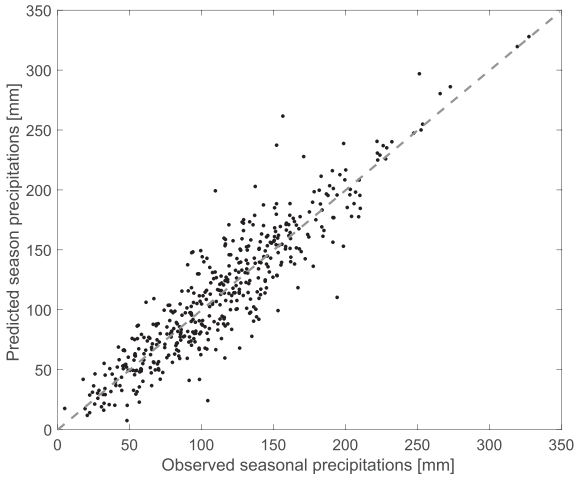

Figure 4. Scatterplot between observed and predicted seasonal precipitation over the full data set.

the western South Indian Ocean along the coasts of Madagascar. Conversely, for the positive phase of NAO, the selected SST are located in the central tropical Pacific Ocean, in a large area of the western Indian Ocean and along the African coasts of the Atlantic Ocean, with a small positively correlated region identified in the western tropical Pacific Ocean. Similarly, SST anomalies negatively correlated with winter precipitation in the positive ENSO phase are mainly located in the central tropical Pacific Ocean, along the coasts of central America, and the Atlantic Ocean along the coasts of central Africa, in the central North Atlantic Ocean, in the eastern Mediterranean Sea, and in large parts of the Indian Ocean. For the negative phase of ENSO, the correlation map illustrates an area of positively correlated SST anomalies in the southern Atlantic Ocean and a small region south of Madagascar. A numerical validation of these teleconnection patterns is reported in section S7 using a complementary data set.

Two interesting insights are evident from this part of the analysis (Table 1 and Figure 3): First, teleconnections from both NAO and ENSO are significant in the Lake Como basin but not equally active in the two phases considered; second, the SST grids characterized by high correlation with Lake Como basin precipitation are largely outside the areas of the Atlantic and Pacific Oceans traditionally considered for monitoring NAO and ENSO variability. These two aspects certainly contribute to the challenge of discovering teleconnection patterns in the Alpine region and the contrasting results reported in the literature, motivating the need for further process-based analysis to fully understand the physical drivers of these teleconnections.

4.2. Precipitation and Streamflow Forecasts

In the second step of the CSI framework (Figure 1), we generate seasonal precipitation forecasts using the ELM forecast model described in section 3.2 to capture the state of multiple climate signals and represent both their asymmetric relationships and their cross-influence with the local hydroclimatic processes (Huang et al., 1998; Mariotti et al., 2002; Matyasovszky, 2003). These model prediction depends on the couple of first PCs extracted from preseason SSTs for the concurrent ENSO and NAO phases, where the average explained variance across signals and phases is 30.4% for the first PC and 19.7% for the second PC. The performance of all 3-month periods (e.g., JFM, FMA, and MAM) predicted precipitation reinitialized at the beginning of each month is illustrated in Figure 4 and demonstrates high forecast accuracy: Pearson correlation coefficient between observed and predicted values is equal to 0.91 over the full data set (i.e., calibration only), and to 0.81 in leave-one-out cross-validation (see Figure S6).

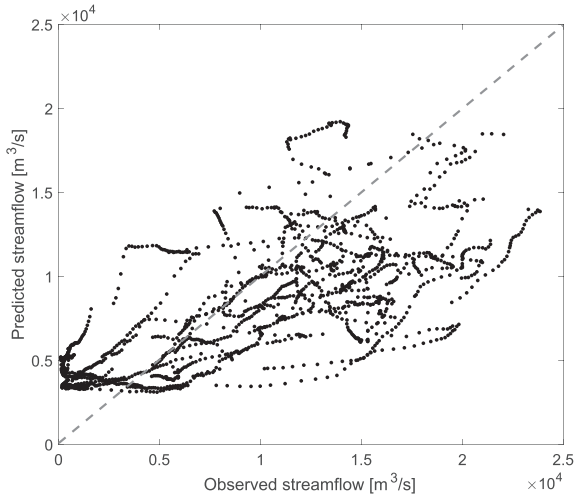

Figure 5. Scatterplot between observed and predicted Lake Como daily inflows cumulated over a lead time of 51 days over the full data set.

The third step of the CSI framework (Figure 1) then transforms these seasonal precipitation forecasts into hydrologic forecasts. This step is performed by first disaggregating the seasonal precipitation forecast into a daily trajectory via kNN resampling to match the concentration time of the basin (~24 hr). Subsequently, the HBV model is run with the disaggregated precipitation forecasts and climatological temperature based on 1990–2003 observations. These simulations produce hydrologic forecasts of Lake Como inflows with a daily temporal resolution for a lead time of 3 months, reinitialized at the beginning of each month as for the precipitation forecasts. The resulting hydrologic forecasts are cumulated over a lead time of 51 days, a time frame demonstrated by Denaro et al. (2017) to be valuable for improving Lake Como operations.

The performance of the resulting streamflow forecasts illustrated in Figure 5 is inferior to the precipitation forecasts (Pearson correlation coefficient equal to 0.71 over the full data set; results in cross-validation are reported in the supporting information), which is likely attributable to the fact that HBV is run with climatological temperature rather than

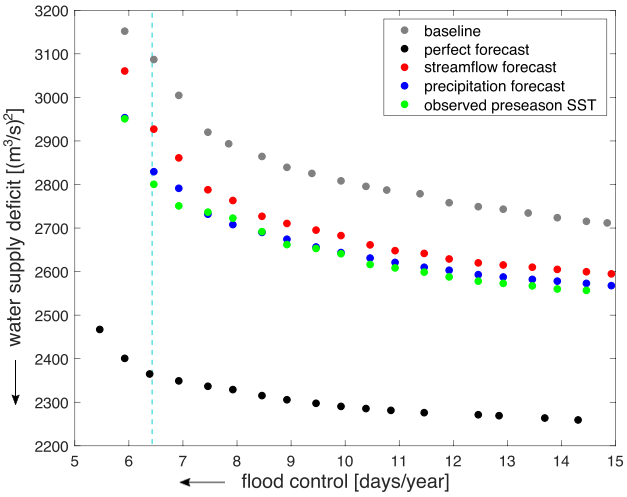

Figure 6. Performance obtained by different Lake Como operating policies informed by streamflow forecasts (red circles), precipitation forecasts (blue circles), or observed preseason SST (green circles). The performance of these solutions is contrasted with the baseline operating policies (gray circles) and with policies informed by perfect forecast (black circles). The arrows indicate the direction of increasing preference for the two objectives, and the cyan dashed line marks the performance of the historical lake regulation in terms of flood control.

predicted temperature. Although temperature is less important than precipitation for generating seasonal hydrological forecasts, it however impacts on the daily streamflow dynamics simulated by the HBV model to match the 24-hr concentration time of the Lake Como catchment.

4.3. Hydrologic Forecast Operational Value

In the final step of the CSI framework (Figure 1), the hydrologic forecasts presented in the previous section are used to inform Lake Como operations. The resulting informed operating policies' performance is illustrated in Figure 6 by the red circles and is compared against an upper-bound solution designed assuming a perfect forecast (black circles) and a baseline solution corresponding to a traditional lake regulation conditioned on the day of the year and the lake level (gray circles). The figure also shows the performance of solutions informed by the precipitation forecast (blue circles) and observed preseason SST (green circles), which will be discussed in the next section. The two axes of the figure represent the two operating objectives (to be minimized), and the arrows indicate the direction of increasing preference, with the best solution located in the bottom-left corner of the figure.

From the observation of the red, gray, and black Pareto fronts, a clear ranking can be made as the three sets of solutions not surprisingly do not intersect. The use of perfect forecasts outperforms other solutions as the (ideal) perfect knowledge of future inflows enables perfect decisions at each time step. The policies using the CSI forecasts, although inferior to the perfect-forecast solutions, are clearly superior to the baseline policies. This gain in performance is attributable to the information provided by the 51-day lead hydrologic forecasts, which result in a significant reduction in irrigation deficit. Conversely, this lead time does not positively contribute to improved flood control. Flood dynamics are on the order of hours to days, requiring much shorter lead times, whereas seasonal irrigation supply is more likely to benefit from seasonal forecasts. However, it is worth mentioning that the downward shift of the red Pareto front generated by the use of the CSI forecasts indirectly influence the performance in flood control as this new set of operating policies allows identifying better compromise alternatives. For example, if looking at the baseline solutions we assume that an acceptable value of J^D might be 2,800 $(m^3/s)^2$, we can see that the informed operating policies attain similar levels of deficit by improving the performance on J^F from 12 to 6–8 flood days per year. The quantitative assessment of the operational value of the hydrologic forecasts is provided by the hypervolume indicator (*HV*, see equation (4)) reported in Table 2. The use of streamflow forecasts increases the baseline *HV* from 0.32 to 0.46, corresponding to a 44% gain in system performance, which is equivalent to about 20% of the maximum improvement attainable using a perfect forecast.

4.4. Operational Value of Precipitation Forecast and Observed Preseason SST

In addition to evaluating the performance of solutions informed by the streamflow forecasts, we assess the performance of operating policies conditioned on seasonal precipitation forecasts (Step 2 of the CSI framework) and observed preseason SST (Step 1 of the CSI framework), illustrated by blue and green circles in Figure 6, respectively. Interestingly, the direct use of seasonal precipitation forecasts—skipping Step 3 of

Table 2
Operational Value of the Hydrologic Forecast, Meteorological Forecasts, and Observed Preseason SST in Terms of Hypervolume Indicator (HV)

Policies	*HV*	Δ*HV*	rel. Δ*HV*
Baseline	0.32	—	—
Streamflow forecast	0.46	0.14	44%
Precipitation forecast	0.50	0.18	56%
Observed preseason SST	0.51	0.19	59%
Perfect forecast	1.00	0.68	212%

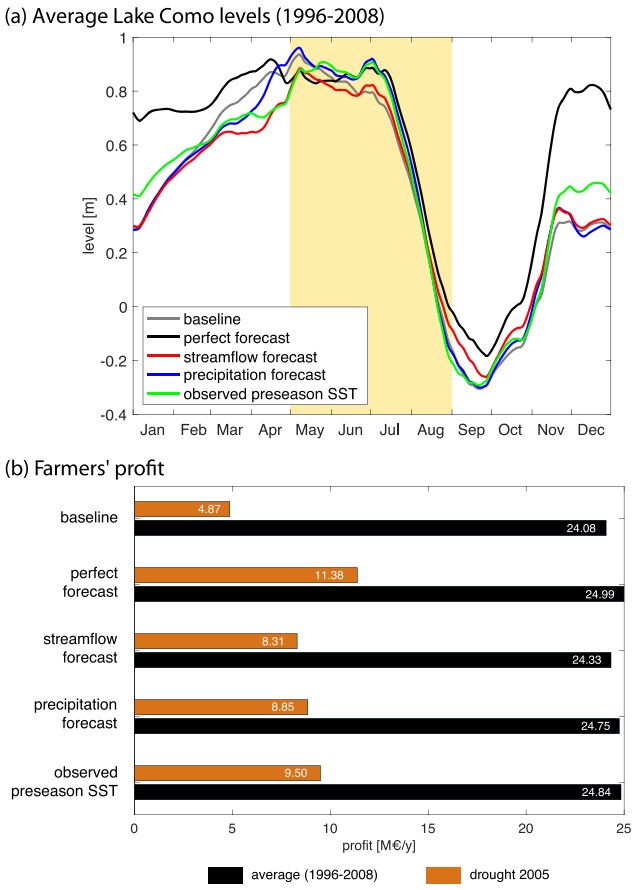

Figure 7. Analysis of the average Lake Como levels (measured with respect to the Malgrate reference level at 197.37 m.a.s.l.) simulated under different selected operating policies (panel a) and corresponding profit of the farmers in the Muzza irrigation district (panel b). The yellow background in the top panel highlights the crop growing period.

CSI—results in a larger reduction of the irrigation supply deficit compared to the streamflow forecast-based solutions. Moreover, only using PCs of observed preseason SST values—skipping both Steps 2 and 3 of CSI—further improves the policy performance.

Numerically, the use of streamflow forecasts improves over the baseline solutions by 44%; this gain increases to 56% and 59% when precipitation forecasts or observed preseason SST are used, respectively. These results suggest that directly informing operational decisions with preseason SST observations selected depending on the climate state (i.e., combination of climate indexes and associated phases) as the main source of local predictability may produce equivalent or superior benefits than those from operational decisions relying on the full CSI modeling chain.

4.5. Analysis of the Operating Policies

To better understand the contribution of streamflow forecasts, precipitation forecasts, and observed preseason SST in improving Lake Como operations, we analyze the dynamic behavior of the system under operating policies that use distinct information. This analysis focuses on the solutions located along the cyan dashed line in Figure 6, which marks the performance of the historical lake regulation in terms of flood control. The rationale of this choice is to look at solutions that reduce the water supply deficit J^D without degrading the performance in J^F, as the historical regulation itself cannot be used as a reference since it also includes additional objectives not accounted for in our model (e.g., hydropower, navigation, fishing, and tourism).

All simulated trajectories of the Lake Como level under each considered policy show a clear annual pattern, with the highest levels observed in late spring due to the snowmelt contribution (Figure 7a). In this period, maximizing the storage while avoiding floods is crucial for supporting the summer drawdown cycle driven by high irrigation demands. The policy conditioned on perfect forecast (black line) is able to maintain the highest level and delay the drawdown. The baseline solution (gray line), which has no information about future inflows, reaches the highest level at the beginning of May but subsequently the level is maintained about 10 cm below the perfect forecast trajectory to have space for buffering potential floods. A similar trajectory is followed by the policy informed by CSI streamflow forecasts (red line), although it is able to further delay the drawdown and to maintain a higher level than the baseline at the end of the agricultural season. Finally, the trajectories obtained under the policies informed by the precipitation forecast (blue line) and observed preseason SST (green line) are able to nearly match the perfect forecast trajectory until the middle of July, further reducing the water supply deficit.

This physical analysis can be translated into economic terms by estimating the agricultural profit for the farmers in the Muzza irrigation district served by Lake Como releases under these operating policies (Figure 7b). Results show the same ranking of solutions obtained in the space of the operating objective (Figure 6) and in the hypervolume indicator (Table 2). All the forecast-based policies increase farmers profit compared with the baseline, which falls shy of about 900,000 €/year with respect to the perfect forecast-based solution. Informing the lake operations with hydrologic forecast produces a 1.0% increase in average profits; this improves further when the precipitation forecast (+2.8%) or observed preseason SST (+3.2%) are used. Interestingly, these benefits are much larger when evaluated over extreme events, such as the drought recorded in 2005, when baseline annual profits dropped to 4.87 M€. This performance is about 20% of the 1996–2008 average baseline profit, and 6.5 M€ less than the expected profits in 2005 under the perfect forecast-based solution. In 2005, the value of the hydrologic forecast, precipitation forecast, and observed preseason SST also grows, producing a 71%, 82%, and 95% increase in farmer profits, respectively. These results suggest a large potential for directly using preseason SST anomalies in predicting and managing extreme droughts.

5. Conclusions

In this paper, we introduce the CSI framework to capture the concurrent state of multiple climate signals and produce seasonal forecasts for informing water reservoir operations. The framework is applied to Lake Como in the Italian lake district, a region where climate teleconnections are still not well understood or completely recognized.

Results indicate the potential of the CSI framework in extending the original NIPA to identify the combined ENSO-NAO climate state, which successfully uncovers notable teleconnection patterns within the Lake Como basin. These newly detected teleconnections are used to generate accurate seasonal precipitation forecasts using multivariate ELMs models, which subsequently feed a HBV model to produce skilful hydrologic forecasts of Lake Como inflows (Pearson correlation coefficients equal to 0.91 and 0.71 for precipitation and streamflow forecasts, respectively). Finally, the forecast operational value is quantified by estimating the difference in system performance between a baseline operating policy relying on traditional information (i.e., day of the year and lake level) with respect to an operating policy informed by the CSI forecasts. Numerical results show that streamflow forecasts produce a 44% improvement in the resulting Pareto optimal solutions. This gain transformed into farmers' profit is, on average, equal to about 250,000 €/year (1% of farmers' average profits) but increases to 3.44 M€ for the extreme drought recorded in 2005 (71% of farmers' profit in that year). Although we can expect this performance to degrade when simulated over out-of-sample data, we believe the policies informed by the CSI forecast will maintain their superiority with respect to the baseline solutions.

In addition, our results suggest that the CSI modeling chain provides intuitive information to improve water system operations but, at the same time, introduces modeling errors that negatively impact the final hydrologic forecast operational value. Overall, the direct use of observed preseason SST anomalies, as identified in the Step 1 of the CSI framework, provide more value than the precipitation or streamflow forecast in informing Lake Como operations, averaging a 3.2% gain in farmer profit and a 95% improvement for the 2005 drought as compared to the baseline solution.

These positive outcomes suggest a number of possible future research directions. Both the precipitation and streamflow forecasts produced by the CSI framework should be benchmarked against existing forecast systems, such as the ECMWF System5 (Johnson et al., 2019) and the European Flood Awareness System (Arnal et al., 2018). Additionally, the identified teleconnection patterns dependent on ENSO and NAO phases motivates a process-based investigation to better understand and clarify the underlying physical processes, perhaps by drawing on global climate model simulations. Extending the CSI framework to additional catchments in diverse hydroclimatic regimes with distinct management challenges is also of interest for better comparing the operational value of the multiple forecast approaches introduced in this paper. Finally, further improvements in system performance are likely achievable by properly combining local hydrologic information with global teleconnections, rather than considering these as alternative sources of information.

Exploring the utility for applying CSI to water reservoir operations under a changing climate is also warranted. In fact, the expected increase in frequency and intensity of extreme events, perhaps resembling the 2005 drought in the Lake Como basin, suggests that extending early actions and decision-making from short to medium and long lead times by means of better forecasts may be increasingly valuable in the future (Turco et al., 2017).

Acknowledgments
We would like to thank Chiara Samale and Alessandro Gentile for their contribution in developing initial numerical experiments. The data used in this study were obtained from IRI Data Library (NOAA's ERSSTV3b), NOAA (MEI index), National Center for Atmospheric Resource (NAO index), Euro4M-APGD (observed precipitation in Lake Como basin), Agenzia Regionale per la Protezione dell'Ambiente (observed temperature in Lake Como basin), and Consorzio dell'Adda (observed Lake Como inflows). The code is available on GitHub: NIPA and ELM (https://github.com/mxgiuliani00/CSI), HBV model (https://github.com/mxgiuliani00/hbv), and Lake Como simulation and EMODPS implementation (https://github.com/mxgiuliani00/LakeComo).

References

Anghileri, D., Voisin, N., Castelletti, A., Pianosi, F., Nijssen, B., & Lettenmaier, D. (2016). Value of long-term streamflow forecasts to reservoir operations for water supply in snow-dominated river catchments. *Water Resources Research*, *52*, 4209–4225. https://doi.org/10.1002/2015WR017864

Arnal, L., Cloke, H., Stephens, E., Wetterhall, F., Prudhomme, C., Neumann, J., et al. (2018). Skilful seasonal forecasts of streamflow over Europe? *Hydrology and Earth System Sciences*, *22*(4), 2057–2072.

Bartolini, E., Claps, P., & D'odorico, P. (2009). Interannual variability of winter precipitation in the European Alps: relations with the North Atlantic Oscillation. *Hydrology and Earth System Sciences*, *13*(1), 17–25.

Beniston, M. (1997). Variations of snow depth and duration in the Swiss Alps over the last 50 years: Links to changes in large-scale climatic forcings, *Climatic change at high elevation sites* (pp. 49–68). Dordrecht: Springer.

Benson, R. (2016). Reviewing reservoir operations: Can federal water projects adapt to change. *Columbia Journal of Environmental Law*, *42*, 353.

Block, P. (2011). Tailoring seasonal climate forecasts for hydropower operations. *Hydrology and Earth System Sciences*, *15*(4), 1355–1368. http://doi.org/10.5194/hess-15-1355-2011

Block, P., & Goddard, L. (2012). Statistical and dynamical climate predictions to guide water resources in Ethiopia. *Journal of Water Resources Planning and Management*, *138*(3), 287–298.

Block, P., & Rajagopalan, B. (2007). Interannual variability and ensemble forecast of Upper Blue Nile Basin Kiremt season precipitation. *Journal of Hydrometeorology*, *8*(3), 327–343.

Brandimarte, L., Di Baldassarre, G., Bruni, G., D'Odorico, P., & Montanari, A. (2011). Relation between the North-Atlantic Oscillation and hydroclimatic conditions in Mediterranean areas. *Water Resources Management*, *25*(5), 1269–1279.

Castelletti, A., Galelli, S., Restelli, M., & Soncini-Sessa, R. (2010). Tree-based reinforcement learning for optimal water reservoir operation. *Water Resources Research*, *46*, W09507. https://doi.org/10.1029/2009WR008898

Castelletti, A., Pianosi, F., & Soncini-Sessa, R. (2008). Water reservoir control under economic, social and environmental constraints. *Automatica*, *44*(6), 1595–1607.

Chiew, F., Zhou, S., & McMahon, T. (2003). Use of seasonal streamflow forecasts in water resources management. *Journal of Hydrology*, *270*(1-2), 135–144.

Cloke, H., & Pappenberger, F. (2009). Ensemble flood forecasting: A review. *Journal of Hydrology*, *375*(3), 613–626.

Dai, A. (2011). Drought under global warming: A review. *Wiley Interdisciplinary Reviews: Climate Change*, *2*(1), 45–65.

Denaro, S., Anghileri, D., Giuliani, M., & Castelletti, A. (2017). Informing the operations of water reservoirs over multiple temporal scales by direct use of hydro-meteorological data. *Advances in Water Resources*, *103*, 51–63. https://doi.org/10.1016/j.advwatres.2017.02.012

Durand, Y., Giraud, G., Laternser, M., Etchevers, P., Mérindol, L., & Lesaffre, B. (2009). Reanalysis of 47 years of climate in the French Alps (1958–2005): Climatology and trends for snow cover. *Journal of applied meteorology and climatology*, *48*(12), 2487–2512.

Efthymiadis, D., Jones, P., Briffa, K., Böhm, R., & Maugeri, M. (2007). Influence of large-scale atmospheric circulation on climate variability in the Greater Alpine Region of Europe. *Journal of Geophysical Research*, *112*, D12104. https://doi.org/10.1029/2006JD008021

Faber, B., & Stedinger, J. (2001). Reservoir optimization using sampling SDP with ensemble streamflow prediction (ESP) forecasts. *Journal of Hydrology*, *249*(1), 113–133. https://doi.org/10.1016/S0022-1694(01)00419-X

Facchi, A., Ortuani, B., Maggi, D., & Gandolfi, C. (2004). Coupled SVAT—Groundwater model for water resources simulation in irrigated alluvial plains. *Environmental Modeling & Software*, *19*(11), 1053–1063.

Folland, C., Knight, J., Linderholm, H., Fereday, D., Ineson, S., & Hurrell, J. (2009). The summer North Atlantic Oscillation: Past, present, and future. *Journal of Climate*, *22*(5), 1082–1103.

Gelati, E., Madsen, H., & Rosbjerg, D. (2011). Stochastic reservoir optimization using El Niño information: Case study of Daule Peripa, Ecuador. *Hydrology Research*, *42*(5), 413–431.

Georgakakos, K., & Graham, N. (2008). Potential benefits of seasonal inflow prediction uncertainty for reservoir release decisions. *Journal of Applied Meteorology and Climatology*, *47*(5), 1297–1321.

Georgakakos, K., Seo, D., Gupta, H., Schaake, J., & Butts, M. (2004). Towards the characterization of streamflow simulation uncertainty through multimodel ensembles. *Journal of Hydrology*, *298*(1-4), 222–241.

Giuliani, M., & Castelletti, A. (2016). Is robustness really robust? How different definitions of robustness impact decision-making under climate change. *Climatic Change*, *135*, 409–424.

Giuliani, M., & Castelletti, A. (2019). Data-driven control of water reservoirs using El Niño Southern Oscillation indexes. In *2019 IEEE International Conference on Environment and Electrical Engineering and 2019 IEEE Industrial and Commercial Power Systems Europe (EEEIC / I CPS Europe)* (pp. 1–5). https://doi.org/10.1109/EEEIC.2019.8783785

Giuliani, M., Castelletti, A., Fedorov, R., & Fraternali, P. (2016). Using crowdsourced web content for informing water systems operations in snow-dominated catchments. *Hydrology and Earth System Sciences*, *20*, 5049–5062. https://doi.org/10.5194/hess-20-5049-2016

Giuliani, M., Castelletti, A., Pianosi, F., Mason, E., & Reed, P. (2016). Curses, tradeoffs, and scalable management: Advancing evolutionary multi-objective direct policy search to improve water reservoir operations. *Journal of Water Resources Planning and Management*, *142*(2), 4015050. https://doi.org/10.1061/(ASCE)WR.1943-5452.0000570

Giuliani, M., Li, Y., Castelletti, A., & Gandolfi, C. (2016). A coupled human-natural systems analysis of irrigated agriculture under changing climate. *Water Resources Research*, *52*, 6928–6947. https://doi.org/10.1002/2016WR019363

Giuliani, M., Pianosi, F., & Castelletti, A. (2015). Making the most of data: An Information Selection and Assessment framework to improve water systems operations. *Water Resources Research*, *51*, 9073–9093. https://doi.org/10.1002/2015WR017044

Grantz, K., Rajagopalan, B., Zagona, E., & Clark, M. (2007). Water management applications of climate-based hydrologic forecasts: case study of the Truckee-Carson River Basin. *Journal of Water Resources Planning and Management*, *133*(4), 339–350.

Grimm, A., & Tedeschi, R. (2009). ENSO and extreme rainfall events in South America. *Journal of Climate*, *22*(7), 1589–1609.

Guariso, G., Orlovski, S., Rinaldi, S., & Soncini-Sessa, R. (1984). An application of the risk-averse approach to the management of lake como. *Journal of Applied Systems Analysis*, *5*(2), 54–64.

Guariso, G., Rinaldi, S., & Soncini-Sessa, R. (1986). The management of Lake Como: A multiobjective analysis. *Water Resources Research*, *22*(2), 109–120. https://doi.org/10.1029/WR022i002p00109

Hadka, D., & Reed, P. (2013). Borg: An auto-adaptive many-objective evolutionary computing framework. *Evolutionary Computation*, *21*(2), 231–259.

Hamlet, A., & Lettenmaier, D. (1999). Columbia River streamflow forecasting based on ENSO and PDO climate signals. *Journal of Water Resources Planning and Management*, *125*(6), 333–341.

Hashimoto, T., Stedinger, J., & Loucks, D. (1982). Reliability, resilience, and vulnerability criteria for water resource system performance evaluation. *Water Resources Research*, *18*(1), 14–20.

Hejazi, M. I., Cai, X., & Ruddell, B. L. (2008). The role of hydrologic information in reservoir operation learning from historical releases. *Advances in Water Resources*, *31*(12), 1636–1650. https://doi.org/10.1016/j.advwatres.2008.07.013

Huang, J., Higuchi, K., & Shabbar, A. (1998). The relationship between the North Atlantic Oscillation and El Niño-Southern Oscillation. *Geophysical Research Letters*, *25*(14), 2707–2710.

Huang, G.-B., Zhu, Q.-Y., & Siew, C.-K. (2006). Extreme learning machine: Theory and applications. *Neurocomputing*, *70*(1), 489–501.

Hurrell, J., & Van Loon, H. (1997). Decadal variations in climate associated with the North Atlantic Oscillation, *Climatic change at high elevation sites* (pp. 69–94). Dordrecht: Springer.

Isotta, F. A., Frei, C., Weilguni, V., Perčec Tadić, M., Lassegues, P., Rudolf, B., et al. (2014). The climate of daily precipitation in the alps: Development and analysis of a high-resolution grid dataset from pan-alpine rain-gauge data. *International Journal of Climatology*, *34*(5), 1657–1675.

Johnson, S., Stockdale, T., Ferranti, L., Balmaseda, M., Molteni, F., Magnusson, L., et al. (2019). SEAS5: The new ECMWF seasonal forecast system. *Geoscientific Model Development*, *12*(3), 1087–1117.

Joliffe, I. (2002). *Principal Component Analysis*. New York, N.Y: Springer.
Kahya, E., & Dracup, J. (1993). US streamflow patterns in relation to the El Niño/Southern Oscillation. *Water Resources Research*, *29*(8), 2491–2503.
Kelman, j., Stedinger, J., Cooper, L., Hsu, E., & Yuan, S. (1990). Sampling stochastic dynamic program ming applied to reservoir operation. *Water Resources Research*, *26*(3), 447–54.
Kim, Y., & Palmer, R. (1997). Value of seasonal flow forecasts in Bayesian stochastic programming. *Journal of Water Resources Planning and Management*, *6*, 327–335. https://doi.org/10.1061/(ASCE)0733-9496(1997)123:6(327)
Kingston, D., Lawler, D., & McGregor, G. (2006). Linkages between atmospheric circulation, climate and streamflow in the northern North Atlantic: Research prospects. *Progress in Physical Geography*, *30*(2), 143–174.
Kingston, D., McGregor, G., Hannah, D., & Lawler, D. (2006). River flow teleconnections across the northern North Atlantic region. *Geophysical Research Letters*, *33*, L14705. https://doi.org/10.1029/2006GL026574
Li, Y., Giuliani, M., & Castelletti, A. (2017). A coupled human-natural system to assess the operational value of weather and climate services for agriculture. *Hydrology and Earth System Sciences*, *21*(9), 4693–4709. https://doi.org/10.5194/hess-21-4693-2017
Libisch-Lehner, C., Nguyen, H., Taormina, R., Nachtnebel, H., & Galelli, S. (2019). On the value of ENSO state for urban water supply system operators: Opportunities, trade-offs, and challenges. *Water Resources Research*, *55*, 2856–2875. https://doi.org/10.1029/2018WR023622
Lindström, G., Johansson, B., Persson, M., Gardelin, M., & Bergström, S. (1997). Development and test of the distributed HBV-96 hydrological model. *Journal of hydrology*, *201*(1-4), 272–288.
López-Moreno, J., Vicente-Serrano, S., Morán-Tejeda, E., Lorenzo-Lacruz, J., Zabalza, J., El Kenawy, A., & Beniston, M. (2011). Influence of Winter North Atlantic Oscillation Index (NAO) on climate and snow accumulation in the mediterranean mountains. In *Hydrological, Socioeconomic and Ecological Impacts of the North Atlantic Oscillation in the Mediterranean Region* (pp. 73–89). Dordrecht: Springer.
Lu, M., Lall, U., Robertson, A. W., & Cook, E. (2017). Optimizing multiple reliable forward contracts for reservoir allocation using multitime scale streamflow forecasts. *Water Resources Research*, *53*, 2035–2050. https://doi.org/10.1002/2016WR019552
Mariotti, A., Zeng, N., & Lau, K.-M. (2002). Euro-Mediterranean rainfall and ENSO—A seasonally varying relationship. *Geophysical Research Letters*, *29*(12), 1621. https://doi.org/10.1029/2001GL014248
Matyasovszky, I. (2003). The relationship between NAO and temperature in Hungary and its nonlinear connection with ENSO. *Theoretical and Applied Climatology*, *74*(1-2), 69–75.
McPhaden, M., Zebiak, S., & Glantz, M. (2006). ENSO as an integrating concept in earth science, *Science*, *314*(5806), 1740–1745.
Nayak, M., Herman, J., & Steinschneider, S. (2018). Balancing flood risk and water supply in California: Policy search integrating short-term forecast ensembles with conjunctive use. *Water Resources Research*, *54*, 7557–7576. https://doi.org/10.1029/2018WR023177
Neitsch, S., Arnold, J., Kiniry, J., & Williams, J. (2011). Soil and water assessment tool theoretical documentation Version 2009 (Tech. Rep. 406). College Station, Texas: Grassland, Soil and Water Research Laboratory–Agricultural Research Service Blackland Research Center–Texas AgriLife Research.
Nowak, K., Prairie, J., Rajagopalan, B., & Lall, U. (2010). A nonparametric stochastic approach for multisite disaggregation of annual to daily streamflow. *Water Resources Research*, *46*, W08529. https://doi.org/10.1029/2009WR008530
Padowski, J., Gorelick, S., Thompson, B., Rozelle, S., & Fendorf, S. (2015). Assessment of human-natural system characteristics influencing global freshwater supply vulnerability. *Environmental Research Letters*, *10*(10), 104014.
Palmer, T., & Hagedorn, R. (2006). *Predictability of weather and climate*. Cambridge: Cambridge University Press.
Poveda, G., Alvarez, D., & Rueda, O. (2011). Hydro-climatic variability over the Andes of Colombia associated with ENSO: A review of climatic processes and their impact on one of the Earth's most important biodiversity hotspots. *Climate Dynamics*, *36*(11-12), 2233–2249.
Rajagopalan, B., Lall, U., Tarboton, D., & Bowles, D. (1997). Multivariate nonparametric resampling scheme for generation of daily weather variables. *Stochastic Hydrology and Hydraulics*, *11*(1), 65–93.
Rodell, M., Famiglietti, J., Wiese, D., Reager, J., Beaudoing, H., Landerer, F., & Lo, M. (2018). Emerging trends in global freshwater availability. *Nature*, *557*, 651–659.
Rolnick, D., Donti, P., Kaack, L., Kochanski, K., Lacoste, A., Sankaran, K., et al. (2019). Tackling climate change with machine learning. *arXiv:1906.05433*.
Sarachik, E., & Cane, M. (2010). *The El Niño-Southern Oscillation phenomenon*. Cambridge: Cambridge University Press.
Scherrer, S., Appenzeller, C., & Laternser, M. (2004). Trends in Swiss Alpine snow days: The role of local-and large-scale climate variability. *Geophysical Research Letters*, *31*, L13215. https://doi.org/10.1029/2004GL020255
Shaman, J. (2014). The seasonal effects of ENSO on European precipitation: Observational analysis. *Journal of Climate*, *27*(17), 6423–6438.
Sharma, A. (2000). Seasonal to interannual rainfall probabilistic forecasts for improved water supply management: Part 3 – A nonparametric probabilistic forecast model. *Journal of Hydrology*, *239*(1), 249–258.
Sharma, A., Luk, K., Cordery, I., & Lall, U. (2000). Seasonal to interannual rainfall probabilistic forecasts for improved water supply management: Part 2—Predictor identification of quarterly rainfall using ocean-atmosphere information. *Journal of Hydrology*, *239*(1), 240–248.
Souza Filho, F., & Lall, U. (2003). Seasonal to interannual ensemble streamflow forecasts for Ceara, Brazil: Applications of a multivariate, semiparametric algorithm. *Water Resources Research*, *39*(11), 1307. https://doi.org/10.1029/2002WR001373
Steduto, P., Hsiao, T., Raes, D., & Fereres, E. (2009). AquaCrop –the FAO crop model to simulate yield response to water: I. concepts and underlying principles. *Agronomy Journal*, *101*(3), 426–437.
Steirou, E., Gerlitz, L., Apel, H., & Merz, B. (2017). Links between large-scale circulation patterns and streamflow in Central Europe: A review. *Journal of hydrology*, *549*, 484–500.
Todini, E. (2014). The role of predictive uncertainty in the operational management of reservoirs. In *Proceedings of the ICWRS2014 Evolving Water Resources Systems: Understanding, Predicting and Managing Water-Society Interactions*, Bologna, Italy, pp. 4–6.
Trenberth, K. (2011). Changes in precipitation with climate change. *Climate Research*, *47*(1–2), 123–138.
Turco, M., Ceglar, A., Prodhomme, C., Soret, A., Toreti, A., & Francisco, J. (2017). Summer drought predictability over europe: Empirical versus dynamical forecasts. *Environmental Research Letters*, *12*(8), 84006.
Turner, S., Bennett, J., Robertson, D., & Galelli, S. (2017). Complex relationship between seasonal streamflow forecast skill and value in reservoir operations. *Hydrology and Earth System Sciences*, *21*(9), 4841–4859.
Ward, P. J., Beets, W., Bouwer, L. M., Aerts, J. C., & Renssen, H. (2010). Sensitivity of river discharge to ENSO. *Geophysical Research Letters*, *37*, L12402. https://doi.org/10.1029/2010GL043215
Ward, P. J., Jongman, B., Kummu, M., Dettinger, M. D., Weiland, F. C. S., & Winsemius, H. C. (2014). Strong influence of el niño southern oscillation on flood risk around the world. *Proceedings of the National Academy of Sciences*, *111*(44), 15,659–15,664.
Wolter, K., & Timlin, M. (1998). Measuring the strength of ENSO events: How does 1997/98 rank? *Weather*, *53*(9), 315–324.

Yuan, X., Wood, E. F., & Ma, Z. (2015). A review on climate-model-based seasonal hydrologic forecasting: physical understanding and system development. *Wiley Interdisciplinary Reviews: Water*, *2*(5), 523–536.

Zanchettin, D., Franks, S., Traverso, P., & Tomasino, M. (2008). On ENSO impacts on European wintertime rainfalls and their modulation by the NAO and the Pacific multi-decadal variability described through the PDO index. *International Journal of Climatology: A Journal of the Royal Meteorological Society*, *28*(8), 995–1006.

Zatarain-Salazar, J., Reed, P., Herman, J., Giuliani, M., & Castelletti, A. (2016). A diagnostic assessment of evolutionary algorithms for multi-objective surface water reservoir control. *Advances in Water Resources*, *92*, 172–185. https://doi.org/10.1016/j.advwatres.2016.04.006

Ziervogel, G., Johnston, P., Matthew, M., & Mukheibir, P. (2010). Using climate information for supporting climate change adaptation in water resource management in South Africa. *Climatic Change*, *103*(3-4), 537–554.

Zimmerman, B. G., Vimont, D. J., & Block, P. J. (2016). Utilizing the state of ENSO as a means for season-ahead predictor selection. *Water Resources Research*, *52*, 3761–3774. https://doi.org/10.1002/2015WR017644

Zitzler, E., Thiele, L., Laumanns, M., Fonseca, C., & da Fonseca, V. (2003). Performance assessment of multiobjective optimizers: An analysis and review. *IEEE Transactions on Evolutionary Computation*, *7*(2), 117–132.